Journal of Solid State Chemistry **168,** 237–244 (2002)
doi:10.1006/jssc.2002.9716

Whitlockite-Related Phosphates $Sr_9A(PO_4)_7$ (*A*=Sc, Cr, Fe, Ga, and In): Structure Refinement of $Sr_9In(PO_4)_7$ with Synchrotron X-Ray Powder Diffraction Data

A. A. Belik,*,[1] F. Izumi,*,[2] T. Ikeda,* M. Okui,† A. P. Malakho,‡ V. A. Morozov,§ and B. I. Lazoryak§

*Advanced Materials Laboratory, National Institute for Materials Science, 1-1 Namiki, Tsukuba, Ibaraki 305-0044, Japan; †Harima Office, Advanced Materials Laboratory, National Institute for Materials Science, 1-1-1 Kouto, Mikazuki-cho, Sayo-gun, Hyogo 679-5198, Japan; ‡Department of Materials Science, Moscow State University, Leninsky Gory, Moscow 119899, Russia; and §Department of Chemistry, Moscow State University, Leninsky Gory, Moscow 119899, Russia

Received April 8, 2002; in revised form June 7, 2002; accepted July 16, 2002

Five phosphates, $Sr_9A(PO_4)_7$ (A = Sc, Cr, Fe, Ga, and In), were synthesized by the solid state method at (1270 to 1420) K and characterized by X-ray powder diffraction, infrared spectroscopy, differential scanning calorimetry, thermogravimetry, and second-harmonic generation (SHG). SHG showed $Sr_9A(PO_4)_7$ to be centrosymmetric. $Sr_9In(PO_4)_7$ is structurally related to β-$Ca_3(PO_4)_2$ (space group $R3c$; a = 10.439 Å and c = 37.375 Å; Z = 21) and $Sr_{9+x}A'_{1.5-x}(PO_4)_7$ (A' = Mn, Fe, Co, Ni, Cu, and Cd; space group $R\bar{3}m$; $a \approx 10.6$ Å and $c \approx 19.7$ Å; Z = 3), having a new type of a monoclinic superstructure. Structure parameters of $Sr_9In(PO_4)_7$ were refined by the Rietveld method from synchrotron X-ray diffraction data on the basis of space group $I2/a$ to afford lattice parameters of a = 18.0425(2) Å, b = 10.66307(4) Å, c = 18.3714(2) Å, and β = 132.9263(5)° (Z = 4). The asymmetric unit of $Sr_9In(PO_4)_7$ contains five Sr, one In, four P, and 14 O sites. Sr^{2+} ions are coordinated to either eight or nine oxide ions. Sr^{2+} ions at an Sr4 site are disordered over two positions near a center of symmetry. In^{3+} ions occupy an octahedral site. O12 atoms belonging to $P1O_4$ tetrahedra are highly disordered because they are bonded to the Sr4 atoms.

Key Words: **phosphate; crystal structure; Rietveld method; X-ray diffraction.**

1. INTRODUCTION

A variety of compounds similar structurally to β-$Ca_3(PO_4)_2$ (1) or whitlockite, $Ca_{18.19}(Mg_{1.17}Fe_{0.83})H_{1.62}(PO_4)_{14}$ (2), have been reported in the literature (3). They include $Ca_3(VO_4)_2$ (4), $Ca_9A(VO_4)_7$ (A = Bi (5) and rare-earth metals (6)), $Ca_3(AsO_4)_2$ (7), $Ca_9A(PO_4)_7$ (A = Sc, Cr, Fe (8), Ga, In (9), and rare-earth metals (10)), $Ca_{9.5}A'(PO_4)_7$ (A' = Mg (11, 12), Co (13), Cu (14, 15), and Zn (16)), $Ca_{3-x}A'_x(PO_4)_2$ (A' = Mg, Mn, Fe, Co, Ni, Cu, Zn, Sr, and Cd (17)), $Ca_9A'A''(PO_4)_7$ (A'' = Li, Na, and K; A' = Mg (18), Ca (19), Mn (20), and Co (21)), and $Ca_{18}A'_2H_2(PO_4)_{14}$ (A' = Mg (22) and Mn (23)). In the above general formulae, A, A', and A'' denote tervalent, bivalent, and univalent metals, respectively.

β-$Ca_3(PO_4)_2$-type compounds (space group $R3c$) have six metal sites, $M1$–$M6$, and three P sites, P1–P3 (3). $M1$, $M2$, $M3$, P2, and P3 occupy general positions (18b) while $M4$, $M5$, $M6$, and P1 are located at 6a sites on the threefold rotation axis. In β-$Ca_3(PO_4)_2$ (M = Ca; a = 10.439 Å and c = 37.375 Å; Z = 21) (1), the Ca1, Ca2, and Ca3 sites in eight-fold coordination and the distorted octahedral Ca5 site are fully occupied by Ca^{2+} ions, the Ca4 site surrounded by nine O atoms is 50% occupied by Ca^{2+} ions, and the $M6$ site is vacant. Smaller cations such as Fe^{3+}, Co^{2+}, and Cu^{2+} are substituted for Ca^{2+} ions at the Ca4 and Ca5 sites in β-$Ca_3(PO_4)_2$ (8, 11–16, 18–23). On the other hand, larger cations, e.g., rare-earth cations, are substituted for Ca^{2+} ions at the Ca1–Ca3 or (Ca1, Ca2, and Ca5) sites (6).

Ferroelectric phase transitions have recently been found in $Ca_9A(PO_4)_7$ (A = Fe and In) (24, 25). Low-temperature forms of $Ca_9A(PO_4)_7$ crystallize in space group $R3c$ with lattice parameters of $a \approx 10.3$ Å and $c \approx 37.3$ Å (Z = 6) in a similar way to β-$Ca_3(PO_4)_2$ (8, 9, 24, 25). In $Ca_9A(PO_4)_7$, the Ca1–Ca3 sites are occupied by Ca^{2+} ions, the $M4$ and $M6$ sites are vacant, and the $M5$ site is occupied by A^{3+} ions. High-temperature forms of $Ca_9A(PO_4)_7$ belong to

[1] Postdoctoral fellow from Department of Chemistry, Moscow State University, Leninsky Gory, Moscow 119899, Russia.

[2] To whom correspondence should be addressed. Fax: +81(298)52-7449. E-mail: IZUMI.Fujio@nims.go.jp.

0022-4596/02 $35.00

space group $R\bar{3}c$, having lattice parameters of $a \approx 10.5$ Å and $c \approx 37.9$ Å (24, 25). In $Ca_9Fe(PO_4)_7$, reversible redox reactions occur without destroying its crystal structure (8, 26). On the reduction of $Ca_9Fe(PO_4)_7$, H atoms are introduced into its crystal lattice to form $Ca_9FeH_x(PO_4)_7$ ($0 < x \leq 1$). Such chemical properties make $Ca_9Fe(PO_4)_7$ promising as a catalyst, a hydrogen-ion conductor, and a material for removing H_2 from gas mixtures (27).

The replacement of Ca^{2+} ions in synthetic whitlockite, $Ca_{18}Mg_2H_2(PO_4)_{14}$ (22), by Sr^{2+} ions yields strontiowhitlockite, $Sr_9Mg(HPO_4)(PO_4)_6$ (28). Wide-range solid solutions with the β-$Ca_3(PO_4)_2$-related structure are formed in a $(Ca,Sr)_3(PO_4)_2$ system (17, 29–31). The high-temperature form of tristrontium bis(phosphate), β-$Sr_3(PO_4)_2$, was regarded as isotypic with β-$Ca_3(PO_4)_2$ (29). Solid solutions, $Sr_{3-x}A'_x(PO_4)_2$ ($A' = Mg$, $0.27 \leq x \leq 1.08$ at 1273 K; $A' = Zn$, $0.27 \leq x \leq 0.81$ at 1298 K (29); $A' = Cd$, $0.36 \leq x \leq 0.63$ at 1273 K (32)), have the β-$Sr_3(PO_4)_2$ structure. $Sr_{9+x}A'_{1.5-x}(PO_4)_7$ ($A' =$ Mn, Fe, Co, Ni, Cu, and Cd) are structurally related to β-$Ca_3(PO_4)_2$ (33–35). These compounds crystallize in space group $R\bar{3}m$ with $a \approx 10.6$ Å and $c \approx 19.7$ Å ($Z = 3$), exhibiting disordered arrangements of $P1O_4$ tetrahadra and Sr^{2+} ions at the Sr3 site (34, 35) corresponding to the $M3$ site in the β-$Ca_3(PO_4)_2$-type structure.

In this work, we have synthesized new strontium metal(III) phosphates $Sr_9A(PO_4)_7$ ($A =$ Sc, Cr, Fe, Ga, and In) where Ca^{2+} ions in $Ca_9A(PO_4)_7$ ($A =$ Sc, Cr, Fe, Ga, and In) (8, 9, 24, 25) are replaced by Sr^{2+} ions. We have found these Sr compounds to have complicated superstructures with lattice parameters of $a \approx 18.0$ Å, $b \approx 10.7$ Å, $c \approx 18.4$ Å, and $\beta \approx 133°$ ($Z = 4$). A measurement of synchrotron X-ray powder diffraction (XRD) data for $Sr_9In(PO_4)_7$ has enabled us to refine its structure parameters and determine disordered arrangements of some Sr, P, and O atoms.

2. EXPERIMENTAL

The five phosphates, $Sr_9A(PO_4)_7$ ($A =$ Sc, Cr, Fe, Ga, and In), were synthesized from mixtures of $SrCO_3$ (99.999%), A_2O_3 (99.9%), and $NH_4H_2PO_4$ (99.999%) with an amount-of-substance ratio of 9:0.5:7. The mixtures were contained in alumina crucibles, heated under air while raising temperature very slowly from room temperature (RT) to 900 K, and allowed to react at 1270–1420 K for 120 h with three intermediated grindings. The products were then quenched to RT. $Sr_9Cr(PO_4)_7$ was light-yellow, $Sr_9Fe(PO_4)_7$ was pink, and the other phosphates, $Sr_9A(PO_4)_7$ ($A =$ Sc, Ga, and In), were white.

Second-harmonic generation (SHG) responses of the powder samples were measured at RT in a reflection scheme. A Q-switch pulsed Nd:YAG laser operated at a wavelength of $\lambda_\omega = 1064$ nm was used as a radiation source with a repetition rate of 4 impulses/s and a duration of impulses of about 12 ns. An incident laser beam was split into two beams to excite the radiation at the halved wavelength, $\lambda_{2\omega}$, of 532 nm simultaneously in the phosphate samples and a reference sample: polycrystalline α-SiO_2. The peak power of the incident beam was about 0.1 MW on a spot 3 mm in diameter on the surface of each sample. No samples of $Sr_9A(PO_4)_7$ showed SHG responses, which presents evidence that $Sr_9A(PO_4)_7$ ($A =$ Sc, Cr, Fe, Ga, and In) are centrosymmetric.

Infrared (IR) spectra were recorded on a Nicolet Magna-750 Fourier spectrometer in a wavenumber ($\tilde{\nu}$) range of 4000–400 cm^{-1} using the KBr pellet technique.

Specific heat capacities, c_p, and changes in mass for $Sr_9A(PO_4)_7$ were measured in air with a NETZSCH STA 409 difference-scanning calorimeter between 293 and 1200 K at a heating rate of 5 K/min. The samples of $Sr_9A(PO_4)_7$ did not show any anomalies in c_p vs T and loss in mass vs T curves.

XRD data of $Sr_9A(PO_4)_7$ were measured at RT with Cu$K\alpha$ radiation on a Rigaku Bragg–Brentano-type powder diffractometer equipped with a diffracted-beam monochromator of curved graphite and operated at 55 kV and 180 mA. The XRD data were collected in a 2θ range from 10 to 60° with a step interval of 0.02° and a counting time of 15 s per step.

Synchrotron XRD data of $Sr_9In(PO_4)_7$ were measured at RT on an ultra-high resolution powder diffractometer (BL15XU at SPring-8) with the Debye–Scherrer geometry using a receiving slit. Incident beams from an undulator were monochromatized to a wavelength of 0.85001 Å with inclined double-crystal monochromators of Si(111). The sample was contained in a quartz-glass capillary tube with an inner diameter of 0.3 mm and rotated at a speed of 6.3 rad/s. The μr (μ: linear absorption coefficient, r: sample radius) value of the sample plus the capillary tube was determined by measuring the transmittance of a direct incident beam to correct for absorption of X-rays. The resulting XRD pattern of $Sr_9In(PO_4)_7$ contained two very weak reflections ($d = 3.226$ and 2.920 Å) due to an unknown impurity. We excluded 2θ ranges corresponding to these two from subsequent Rietveld refinements.

Structure parameters of $Sr_9In(PO_4)_7$ were refined by the Rietveld method from the synchrotron XRD data using RIETAN-2000 (36). The split pseudo-Voigt function of Toraya (37) was fit to each reflection profile, and a composite background function to the background. The composite background function was an 11th-order Legendre polynomial multiplied by a set of numerical values to approximate the background. The approximate background spectrum was determined with PowderX (38). Coefficients for analytical approximation to atomic scattering factors for Sr, In, P, and O were taken from Ref. (39). Their anomalous scattering factors were evaluated

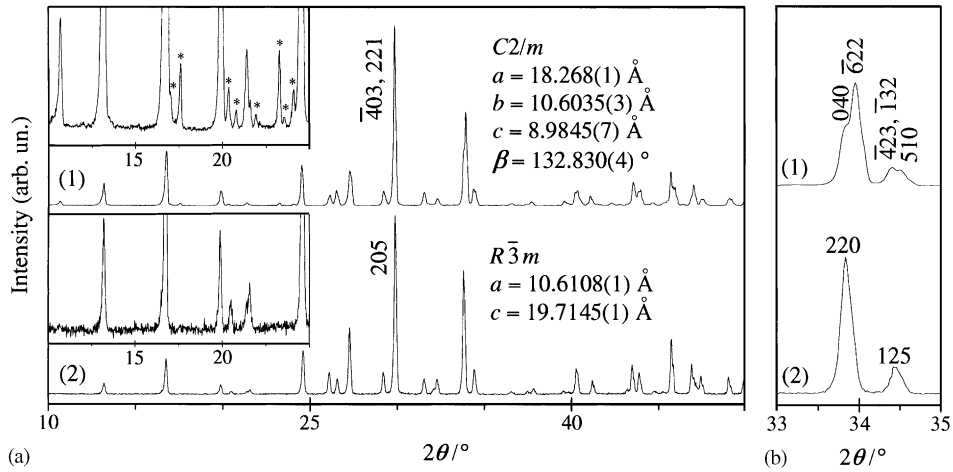

FIG. 1. XRD patterns of (1) $Sr_9Fe(PO_4)_7$ and (2) $Sr_9Fe_{1.5}(PO_4)_7$ in 2θ ranges (a) from 10° to 50° and (b) from 33° to 35° with indices for some reflections. Asterisks in the inset indicate superstructure reflections in $Sr_9Fe(PO_4)_7$.

with a computer program CROMER by the Cromer–Liberman method adopting a Kissel–Pratt correction (40). Isotropic atomic displacement parameters, U, with the isotropic Debye–Waller factor represented as exp $(-8\pi^2 U \sin^2\theta / \lambda^2)$ were assigned to all the sites.

3. RESULTS AND DISCUSSION

3.1. Characterization of the Products

XRD patterns of $Sr_9A(PO_4)_7$ (A = Sc, Cr, Fe, Ga, and In) were very similar to those of $Sr_{9+x}A'_{1.5-x}(PO_4)_7$ (A' = Mn, Fe, Co, Ni, Cu, and Cd) (33–35). However, some reflections, e.g., a reflection near $2\theta \approx 34°$, in the XRD patterns of $Sr_9A(PO_4)_7$ were split in contrast with those of $Sr_{9+x}A'_{1.5-x}(PO_4)_7$, as exemplified for A and A' = Fe in Fig. 1.

We found that the splitting of the reflections arises from the lowering of the crystallographic symmetry from a trigonal system in $Sr_{9+x}A'_{1.5-x}(PO_4)_7$ to a monoclinic one in $Sr_9A(PO_4)_7$. The hexagonal (h) unit-cell (space group $R\bar{3}m$, No. 166; $a_h \approx 10.6$ Å and $c_h \approx 19.7$ Å) for $Sr_{9+x}A'_{1.5-x}(PO_4)_7$ (34, 35) can be transformed into a monoclinic (m) one in such a way that $\boldsymbol{a}_m = \boldsymbol{a}_h - \boldsymbol{b}_h$, $\boldsymbol{b}_m = \boldsymbol{a}_h + \boldsymbol{b}_h$, and $\boldsymbol{c}_m = (-\boldsymbol{a}_h + \boldsymbol{b}_h + \boldsymbol{c}_h)/3$. This transformation gives centrosymmetric space group $C1\ 2/m\ 1$ (No. 12, unique axis b, cell choice 1) (41) and lattice parameters of $a_m \approx 18.4$ Å, $b_m \approx 10.6$ Å, $c_m \approx 8.98$ Å, and $\beta_m \approx 133°$ ($Z = 2$). In what follows, $C1\ 2/m\ 1$ will be abbreviated as $C2/m$. All the reflections with intensity ratios, I/I_1, greater than ca. 0.01 (I: peak intensity, I_1: peak intensity of the strongest profile for 221 and $\bar{4}03$ reflections) in the XRD patterns of $Sr_9A(PO_4)_7$ were indexed on the basis of this monoclinic unit-cell. However, the XRD patterns of $Sr_9A(PO_4)_7$ exhibited several additional reflections that could be indexed in a monoclinic cell with $a'_m = a_m$, $b'_m = b_m$, $c'_m = 2c_m$, and $\beta'_m = \beta_m (Z = 4)$.

Because of the limited number of the observed superlattice reflections (Fig. 1a), the lattice parameters of $Sr_9A(PO_4)_7$ were refined by the Rietveld method on the basis of the subcell with space group $C2/m$ and a structural model derived from the crystal data of $Sr_9Fe_{1.5}(PO_4)_7$ (35). Table 1 lists refined lattice parameters of $Sr_9A(PO_4)_7$, showing that the ionic radii, r, of A^{3+} ions in sixfold coordination (42) and unit-cell volumes, V, are strongly correlated.

IR spectra of $Sr_9A(PO_4)_7$ (A = Fe and In) (Fig. 2) showed a series of absorption bands assigned to P–O stretching,

TABLE 1
Lattice Parameters for $Sr_9A(PO_4)_7$ (A = Sc, Cr, Fe, Ga, and In) in the $C2/m$ Model

A^{3+}	$r(A^{3+})$ (Å)	a (Å)	b (Å)	c (Å)	β (deg)	V (Å^3)
Cr	0.615	18.252(2)	10.5763(6)	8.9747(9)	132.774(8)	1271.7(2)
Ga	0.620	18.237(3)	10.5809(6)	8.978(1)	132.752(8)	1272.1(3)
Fe	0.645	18.268(1)	10.6035(3)	8.9845(7)	132.830(4)	1276.3(1)
Sc	0.745	18.345(3)	10.6509(5)	9.008(1)	132.929(7)	1288.8(3)
In	0.800	18.365(2)	10.6607(4)	9.019(1)	132.917(6)	1293.2(2)

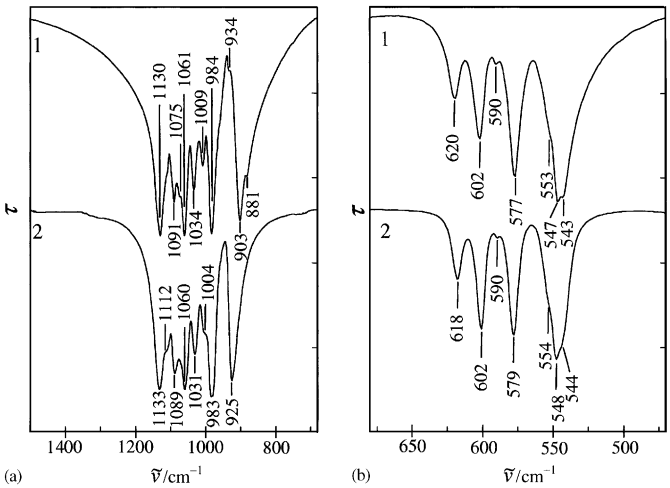

FIG. 2. IR spectra in wavenumber, $\tilde{\nu}$, regions of (a) 1500–680 cm^{-1} and (b) 680–470 cm^{-1} for (1) $Sr_9Fe(PO_4)_7$ and (2) $Sr_9In(PO_4)_7$. τ: transmittance (arbitrary unit).

ν(P–O), and O–P–O bending, δ(O–P–O), vibrations at 1300–800 cm^{-1} and 650–500 cm^{-1}, respectively. The IR spectra were very similar to each other but differed considerably from those of $Sr_{9+x}A'_{1.5-x}(PO_4)_7$ (35). These findings provided evidence that PO_4 tetrahedra in $Sr_9A(PO_4)_7$ and $Sr_{9+x}A'_{1.5-x}(PO_4)_7$ have different chemical environments.

3.2. Structure Refinement of $Sr_9In(PO_4)_7$

With the monoclinic superlattice of $a \approx 18.37$ Å, $b \approx 10.66$ Å, $c \approx 18.04$ Å, and $\beta \approx 132.93°$, reflection conditions in $Sr_9In(PO_4)_7$ were found to be $h+k+l=2n$ for hkl, and $h=2n$ and $l=2n$ for $h0l$, affording possible space groups $I1a1$ (No. 9, unique axis b, cell choice 3) and $I1\ 2/a\ 1$ (No. 15, unique axis b, cell choice 3) (41). Because $I1a1$ is noncentrosymmetric, $Sr_9In(PO_4)_7$ belongs to $I1\ 2/a\ 1$. From now on, $I1\ 2/a\ 1$ will be abbreviated to $I2/a$. Selected-area electron diffraction has also offered conclusive evidence that $Sr_9A(PO_4)_7$ has space group $I2/a$ (43).

With the lattice transformation $\boldsymbol{a}'_m = \boldsymbol{a}_m, \boldsymbol{b}'_m = \boldsymbol{b}_m$, and $\boldsymbol{c}'_m = 2\boldsymbol{c}_m$, fractional coordinates in space group $C2/m$ were first converted to those in space group $I1\ 2/c\ 1$ (No. 15, unique axis b) (41). The resulting fractional coordinates were further transformed to those in space group $I2/a$ with a lattice transformation $\boldsymbol{a}''_m = \boldsymbol{c}'_m, \boldsymbol{b}''_m = -\boldsymbol{b}'_m$, and $\boldsymbol{c}''_m = \boldsymbol{a}'_m$.

In early stages of Rietveld refinements with space group $I2/a$, linear constraints were imposed on half of fractional coordinates and U parameters for P and O atoms derived from the same atoms in the $C2/m$ model: $x_2 = x_1 + 0.5$, $y_2 = y_1, z_2 = z_1$, and $U_2 = U_1$, where each pair of $(x_1, x_2), (y_1, y_2), (z_1, z_2)$, and (U_1, U_2) was assigned to (P3, P4), (O22, O23), (O31, O43), (O32, O42), (O33, O44), and (O34, O41) atoms.

A Rietveld refinement into which the above constraints were introduced was successful in view of the resulting R factors, U parameters, interatomic distances, and bond angles. When the Sr4 atom was located at an ideal 4b site (0, $\frac{1}{2}$, 0; Sr4′) on an inversion center with the occupancy, g, of unity, U(Sr4′) converged to 4.42(7) nm^2. The Sr4 atom was, therefore, displaced slightly from the 4b position to a general position (8f). At the last stage of the refinement, the following linear constraints were imposed on U parameters: $U(O23) = U(O22)$, $U(O41) = U(O34)$, $U(O43) = U(O31)$, and $U(O44) = U(O33)$. The other constraints were no longer imposed at this stage. Partial profile relaxation (36) was applied to $\bar{6}04$, 222, $\bar{4}26$, and 040 reflections to improve fits in these reflections in the final structure refinement. An 8f site (0.045, 0, 0.365; Sr6) corresponding to the $M4$ and $M6$ sites in the β-$Ca_3(PO_4)_2$-type structure proved to be vacant in $Sr_9In(PO_4)_7$ in a similar manner to the $M4$ and $M6$ sites in $Ca_9In(PO_4)_7$ (25).

Table 2 lists experimental/refinement conditions, final R factors, lattice parameters, and so forth. Final fractional coordinates and U values are listed in Table 3, and metal–oxygen bond lengths, l, in Table 4. Figure 3 displays observed, calculated, and difference XRD patterns of $Sr_9In(PO_4)_7$ for the $I2/a$ model. The very small standard

TABLE 2
Conditions of the XRD Experiments and Parts of Refinement Conditions and Results for $Sr_9In(PO_4)_7$

λ (Å)	0.85001
2θ range (deg)	2.5–64
Scan width (deg)	0.003
Number of data points	20504
Space group	$I2/a$ (No. 15, cell choice 3)
Z	4
Lattice parameters	
a (Å)	18.0425(2)
b (Å)	10.66307(4)
c (Å)	18.3714(2)
β (deg)	132.9263(5)
V (Å^3)	2588.02(4)
Number of Bragg reflections	2627
Variables	
Structure/lattice	88/4
Background/profile	12/10
peak shift/scale	1/1
PPP[a]	17
R_{wp}, R_p	5.42%, 4.15%
R_B, R_F	2.00%, 1.64%
S[b]	0.74

[a] Refined primary profile parameters (36).
[b] $S = R_{wp}/R_e$.

TABLE 3
Fractional Coordinates and Isotropic Atomic Displacement Parameters for $Sr_9In(PO_4)_7$ in the $I2/a$ Model

Atom	Site	g	x	y	z	U (nm^2)
Sr1	8f	1	0.19632(7)	0.00224(14)	0.28165(6)	0.65(3)
Sr2	8f	1	0.30507(8)	0.72200(11)	0.44279(7)	0.63(3)
Sr3	8f	1	0.80288(8)	0.71643(11)	0.44268(7)	0.63(3)
Sr4	8f	$\frac{1}{2}$	0.0133(2)	0.5006(4)	−0.0067(2)	0.67(5)
Sr5	8f	1	−0.01492(8)	0.73053(10)	0.23355(7)	1.04(3)
In	4a	1	0	0	0	0.60(2)
P1	4e	1	$\frac{1}{4}$	0.4789(5)	0	2.41(12)
P2	8f	1	0.4028(2)	−0.0039(4)	0.1088(2)	0.62(6)
P3	8f	1	0.0977(2)	0.2621(3)	0.1515(2)	0.79(9)
P4	8f	1	0.5960(2)	0.2585(3)	0.1529(2)	0.53(8)
O11	8f	1	0.8229(4)	0.6111(5)	0.0902(4)	1.4(2)
O12	8f	1	0.2013(6)	0.9508(7)	0.5253(5)	9.6(4)
O21	8f	1	0.4854(4)	0.0018(7)	0.7931(3)	0.09(13)
O22	8f	1	0.3536(5)	0.8704(6)	0.1018(4)	0.12(10)[a]
O23	8f	1	0.8514(5)	0.8889(6)	0.1017(5)	0.12[a]
O24	8f	1	0.3938(4)	−0.0015(7)	0.0177(3)	0.37(13)
O31	8f	1	0.3503(4)	0.2552(6)	0.2419(4)	0.14(9)[b]
O32	8f	1	0.8540(5)	0.8604(6)	0.3673(5)	0.6(2)
O33	8f	1	0.6076(5)	0.6353(6)	0.6177(5)	0.22(9)[c]
O34	8f	1	0.5157(5)	0.2021(6)	0.4139(4)	0.63(9)[d]
O41	8f	1	0.0137(5)	0.2044(6)	0.4107(4)	0.63[d]
O42	8f	1	0.3466(5)	0.8612(6)	0.3542(5)	0.2(2)
O43	8f	1	0.8542(4)	0.2609(6)	0.2377(4)	0.14[b]
O44	8f	1	0.1053(5)	0.6307(6)	0.6149(5)	0.22[c]

[a–d] These parameters were constrained to be equal to each other.

deviations for the lattice parameters and S less than 1 are believed to arise form the large number of data points, 20,504, and the use of a conventional formula to calculate estimated standard deviations of refinable parameters.

3.3. Structural Properties of $Sr_9In(PO_4)_7$

The crystal structure of $Sr_9In(PO_4)_7$ comprises two types of layers perpendicular to the b-axis: layers I and II (Fig. 4). Figure 5 illustrates projections of these layers along the [010] direction with the pseudo-hexagonal unit cell expressed with dotted lines. The crystal structures of $Ca_9In(PO_4)_7$ and $Sr_9Fe_{1.5}(PO_4)_7$ also consist of similar layers: layers I and II (25, 35) (Fig. 6). In all the compounds, layers I contain only B-type columns whereas layers II contain both A- and B-type columns, where columns A are represented as $[P1O_4–M4–M5–M6–]_\infty$, and columns B as $[PO_4–PO_4–M1–M3–M2–]_\infty$ in the β-$Ca_3(PO_4)_2$-type structure (Figs. 6a and 6c).

Figures 5 and 6 clearly show that $Ca_9In(PO_4)_7$, $Sr_9Fe_{1.5}(PO_4)_7$, and $Sr_9In(PO_4)_7$ are structurally very similar to each other but different in positions of cations and orientations of phosphate ions. These figures also present relations among different sites in the three compounds. In $Sr_9Fe_{1.5}(PO_4)_7$, the Sr1, Sr3, Fe4, and Fe5 sites correspond to the ($M1$, $M2$), $M3$, ($M4$, $M6$), and $M5$ sites in the β-$Ca_3(PO_4)_2$-type structure, respectively. The ($M1$, $M2$), $M3$, ($M4$, $M6$), and $M5$ sites, in turn, correspond to the (Sr1, Sr2, Sr3), (Sr4, Sr5), Sr6, and In sites in $Sr_9In(PO_4)_7$, respectively.

The orientations of the $P1O_4$ tetrahedra differ noticeably among these structures. The $P1O_4$ tetrahedron in $Ca_9In(PO_4)_7$ is ordered with the P1 and O11 atoms laid on the threefold rotation axis (Fig. 6a). The $P1O_4$ tetrahedron in $Sr_9Fe_{1.5}(PO_4)_7$ is disordered. That is, the P1 atom is situated at the center of symmetry on the threefold rotation axis while the O atoms are bonded to the P1 atom off this

TABLE 4
Bond Lengths l in $Sr_9In(PO_4)_7$

Bonds	l (Å)	Bonds	l (Å)
Sr1–O42	2.544(7)	Sr4–O32	2.484(8)
Sr1–O21	2.550(5)	Sr4–O32a	2.599(8)
Sr1–O32	2.573(7)	Sr4–O42	2.601(7)
Sr1–O33	2.662(7)	Sr4–O34	2.614(8)
Sr1–O31	2.663(6)	Sr4–O41	2.664(8)
Sr1–O43	2.672(7)	Sr4–O42a	2.705(7)
Sr1–O44	2.691(7)	Sr4–O34a	3.009(7)
Sr1–O12	2.715(7)	Sr4–O41a	3.040(7)
Sr1–O11	2.850(6)	Sr4–O12	3.068(7)
		Sr4—Sr4a[a]	0.671(3)
Sr2–O12	2.530(7)	Sr5–O31	2.544(6)
Sr2–O43	2.539(6)	Sr5–O23	2.565(6)
Sr2–O34	2.539(6)	Sr5–O11	2.573(6)
Sr2–O22	2.577(7)	Sr5–O43	2.590(6)
Sr2–O22a	2.605(6)	Sr5–O22	2.606(6)
Sr2–O24	2.643(7)	Sr5–O21	2.672(7)
Sr2–O44	2.650(6)	Sr5–O41	2.680(6)
Sr2–O42	2.661(6)	Sr5–O21a	3.040(7)
		Sr5–O34	3.052(6)
Sr3–O31	2.558(5)	In–O44 (× 2)	2.131(7)
Sr3–O23	2.566(7)	In–O24 (× 2)	2.151(5)
Sr3–O41	2.603(6)	In–O33 (× 2)	2.193(7)
Sr3–O32	2.620(7)	Sr4′[b]–O32 (× 2)	2.520
Sr3–O24	2.629(7)	Sr4′–O42 (× 2)	2.633
Sr3–O33	2.650(6)	Sr4′–O34 (× 2)	2.799
Sr3–O11	2.652(5)	Sr4′–O41 (× 2)	2.838
Sr3–O23a	2.659(7)	Sr4′–O12 (× 2)	3.374
Sr3–O11a	3.087(6)		
P1–O12 (× 2)	1.451(7)	P2–O23	1.488(7)
P1–O11 (× 2)	1.559(6)	P2–O21	1.538(5)
		P2–O22	1.564(7)
		P2–O24	1.567(4)
P3–O31	1.499(6)	P4–O41	1.513(6)
P3–O32	1.544(7)	P4–O43	1.559(6)
P3–O33	1.548(6)	P4–O42	1.572(7)
P3–O34	1.558(7)	P4–O44	1.591(6)

[a] Interatomic distance between split positions.
[b] Sr4′ is the ideal position (4b; 0, $\frac{1}{2}$, 0) corresponding to the Sr4 site.

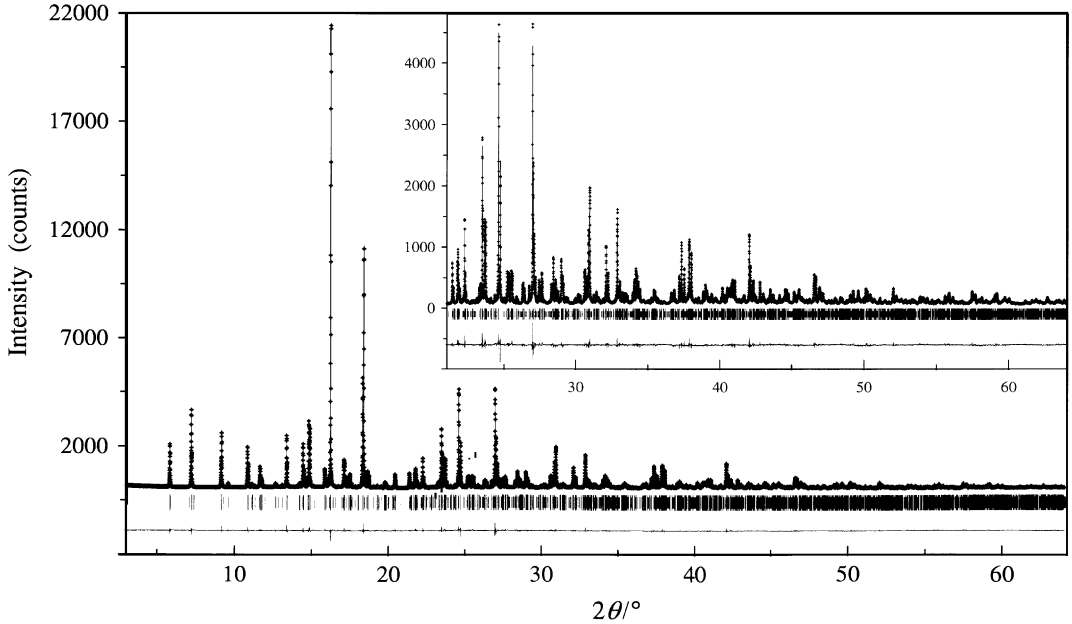

FIG. 3. Observed (crosses), calculated (solid line), and difference synchrotron XRD patterns obtained for $Sr_9In(PO_4)_7$ with the $I2/a$ model. Bragg reflections are indicated by tick marks with shorter ones given for superlattice reflections. The inset shows Rietveld refinement profiles in a 2θ region from 21° to 64°.

axis (Fig. 6b). In $Sr_9In(PO_4)_7$, $P1O_4$ tetrahedra are orientationally ordered, but both P and O atoms in the phosphate ions are displaced from a pseudo-threefold rotation axis (Fig. 5a).

The Ca1, Ca2, and Ca3 sites in $Ca_9In(PO_4)_7$ are fully occupied by Ca^{2+} ions (Figs. 6a and 6c). In $Sr_9Fe_{1.5}(PO_4)_7$, Sr1 atoms are ordered, but Sr3 atoms are split into four pieces. In $Sr_9In(PO_4)_7$, Sr1, Sr2, Sr3, and Sr5 atoms are ordered whereas Sr4 atoms are split into two pieces near the center of symmetry. As discussed above, all the atoms on layer I are ordered in $Sr_9In(PO_4)_7$ (Fig. 5b) as in $Ca_9In(PO_4)_7$ (Fig. 6c). Layers II (Fig. 5a) in $Sr_9In(PO_4)_7$ include some disordered atoms as in $Sr_9Fe_{1.5}(PO_4)_7$ (Fig. 6b).

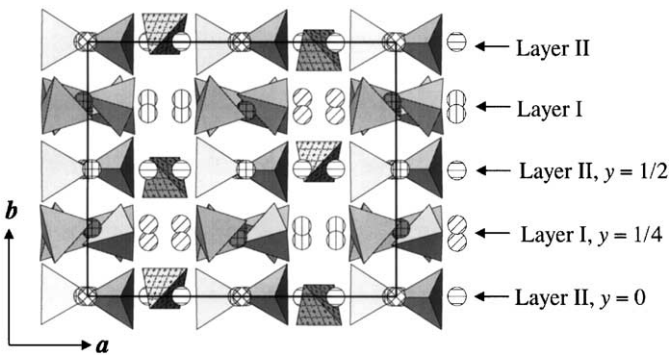

FIG. 4. Crystal structure of $Sr_9In(PO_4)_7$ viewed along the [001] direction. Layers I and II are marked with arrows.

Figure 7 displays projections of $Sr4'O_{10}$, $Sr5O_9$, and $P1O_4$ polyhedra along the [010] direction. The $Sr4'O_{10}$ polyhedra include two O12 atoms and four PO_4 edges (O32–O34, O32–O34, O41–O42, and O41–O42). The $Sr4'O_{10}$ polyhedra are elongated along the [100] direction with l(Sr4′–O12) = 3.374 Å (× 2) (Table 4). Such distortion in the $Sr4'O_{10}$ polyhedra is responsible for the static displacements of the Sr^{2+} ions from the centers of the polyhedra toward one of the O12 atoms. The off-center

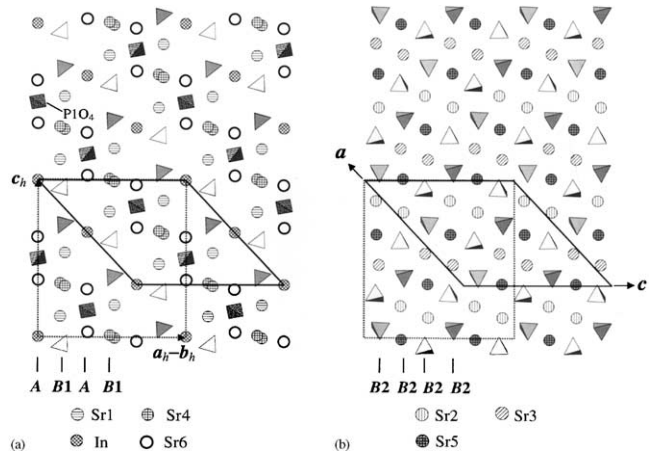

FIG. 5. Layers (a) II and (b) I in $Sr_9In(PO_4)_7$ with the b-axis perpendicular to this page. Dotted lines present the pseudo-hexagonal unit-cell, and columns A and B are marked with ticks. Positions Sr4 are split into two pieces.

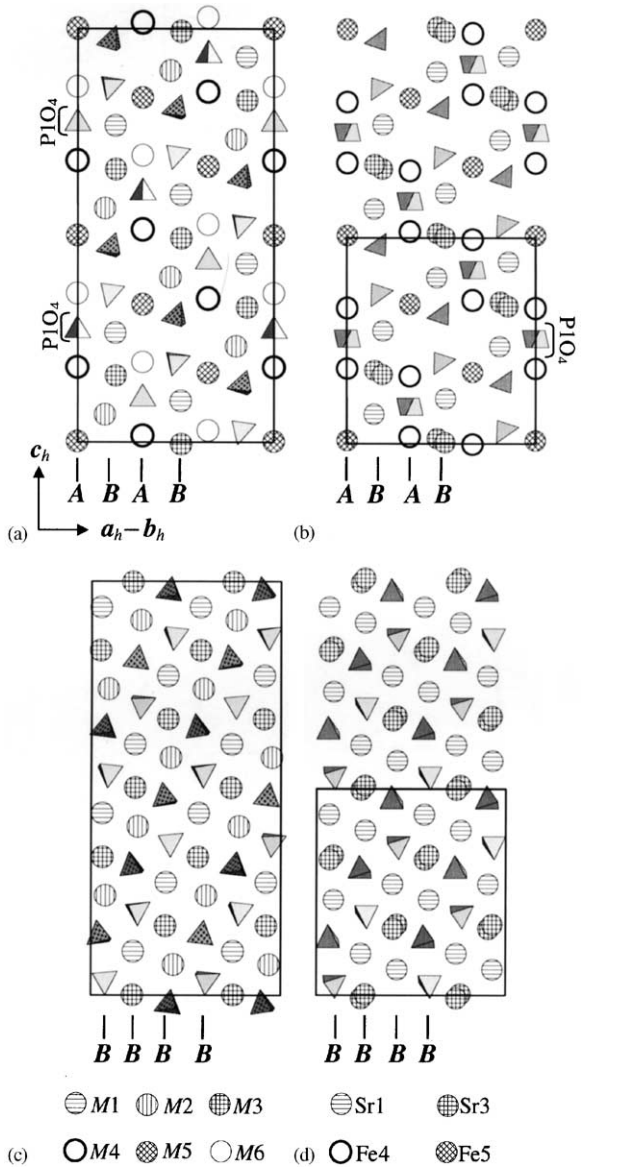

FIG. 6. Projection of layers II (a, b) and layers I (c, d) in $Ca_9In(PO_4)_7$ (β-$Ca_3(PO_4)_2$-type structure) (a, c) and $Sr_9Fe_{1.5}(PO_4)_7$ (b, d) along the [110] direction. Columns *A* and *B* are marked with ticks, and solid lines represent unit-cells. The disordered $P1O_4$ tetrahedra and split positions Sr3 are shown for $Sr_9Fe_{1.5}(PO_4)_7$.

shifts of the Sr4 atom give a smaller distance, *l*(Sr4–O12) = 3.068 Å, for one O12 atom and a much larger distance, *l*(Sr4–O12) = 3.686 Å, for another O12 atom. Consequently, the coordination number of Sr4 becomes nine.

The apparently large *U*(O12) value of 9.6 nm^2 evidently reflects disordering of Sr4 atoms. Half of O12 atoms are bonded to Sr4 atoms while the remaining half of O12 atoms do not form any bonds to these Sr atoms. The disordering of the O12 atoms necessarily leads to that of the $P1O_4$ tetrahedra containing O12. The disordered

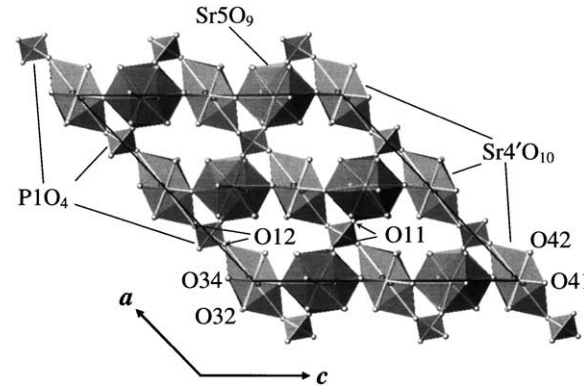

FIG. 7. $Sr4'O_{10}$ and $Sr5O_9$ polyhedra and $P1O_4$ tetrahedra viewed along the [010] direction. Split Sr4 atoms are represented with black circles.

arrangements of the $P1O_4$ tetrahedra are partly absorbed into the much larger *U* value of 2.41(12) nm^2 for the P1 atom in comparison with those for other P atoms (0.5–0.8 nm^2). Simultaneous refinement of *g* and *U* for the O12 atom gave $g = 1.039(8)$ and $U = 11.1(5)$ nm^2, which supports the idea that the O12 site is fully occupied.

The present study has successfully clarified the details in the complicated monoclinic superstructure of $Sr_9In(PO_4)_7$. The asymmetric unit of $Sr_9In(PO_4)_7$ includes 24 sites: five sites of Sr^{2+} ions coordinated to either eight or nine O atoms, one octahedral site of In^{3+} ions, four P atoms, and 14 O sites. An instrumental resolution at the top international level attained in the synchrotron X-ray powder diffractometer and the excellent ability of RIETAN-2000 to deal with complex crystal structures made it possible to construct the structural model of $Sr_9In(PO_4)_7$, refine its structure parameters, and determine the disordered arrangements of Sr4, P1, and O12 atoms. Work is now under way to apply this combination of the diffractometer and pattern-fitting system to another phosphate with much more disordered atomic arrangements.

ACKNOWLEDGMENTS

This work was partially supported by the Russian Foundation for Basic Research (Grants 00-03-32660, 01-03-06121, 01-03-06122, and 01-03-06123) and the Interdisciplinary Scientific Project of Moscow State University (Grant No. 21). A.A.B. acknowledges the award of the STA Fellowship from the Japan Science and Technology Corporation. We thank the staff of beam line BL15XU at SPring-8 for technical assistance and Dr. S. Yu. Stefanovich of Moscow State University for the SHG measurements.

REFERENCES

1. B. Dickens, L. W. Schroeder, and W. E. Brown, *J. Solid State Chem.* **10,** 232–248 (1974).

2. C. Calvo and R. Gopal, *Am. Mineral.* **60,** 120–133 (1975).
3. B. I. Lazoryak, *Russ. Chem. Rev.* **65,** 307–325 (1996). [Eng. Trans. 287–305]
4. R. Gopal and C. Calvo, *Z. Kristallogr.* **137,** 67–85 (1973).
5. J. S. O. Evans, J. Huang, and A. W. Sleight, *J. Solid State Chem.* **157,** 255–260 (2001), doi:10.1006/jssc.2000.9045.
6. A. A. Belik, S. V. Grechkin, L. O. Dmitrienko, V. A. Morozov, S. S. Khasanov, and B. I. Lazoryak, *Crystallogr. Rep.* **45,** 896–901 (2000).
7. R. Gopal and C. Calvo, *Can. J. Chem.* **49,** 1036–1046 (1971).
8. B. I. Lazoryak, V. A. Morozov, A. A. Belik, S. S. Khasanov, and V. Sh. Shekhtman, *J. Solid State Chem.* **122,** 15–21 (1996), doi:10.1006/jssc.1996.0074.
9. V. N. Golubev, B. N. Viting, O. B. Dogadin, and B. I. Lazoryak, *Russ. J. Inorg. Chem.* **35,** 3037–3041 (1990).
10. V. N. Golubev and B. I. Lazoryak, *Izv. Akad. Nauk SSSR, Neorg. Mater.* **27,** 576–579 (1991).
11. L. W. Schroeder, B. Dickens, and W. E. Brown, *J. Solid State Chem.* **22,** 253–262 (1977).
12. A. Bigi, G. Falini, E. Foresti, A. Ripamonti, M. Gazzano, and N. Roveri, *Z. Kristallogr.* **211,** 13–16 (1996).
13. A. A. Belik, V. A. Morozov, S. S. Khasanov, and B. I. Lazoryak, *Mater. Res. Bull.* **33,** 987–995 (1998).
14. N. Khan, V. A. Morozov, S. S. Khasanov, and B. I. Lazoryak, *Mater. Res. Bull.* **32,** 1211–1220 (1997).
15. A. A. Belik, O. V. Yanov, and B. I. Lazoryak, *Mater. Res. Bull.* **36,** 1863–1871 (2001).
16. R. J. B. Jakeman, A. K. Cheetham, N. J. Clayden, and C. M. Dobson, *J. Solid State Chem.* **78,** 23–34 (1989).
17. A. G. Nord, *Neues Jahrb. Mineral. Monatsh.* **11,** 489–497 (1983).
18. V. A. Morozov, I. A. Presnyakov, A. A. Belik, S. S. Khasanov, and B. I. Lazoryak, *Crystallogr. Rep.* **42,** 758–769 (1997).
19. V. A. Morozov, A. A. Belik, R. N. Kotov, I. A. Presnyakov, S. S. Khasanov, and B. I. Lazoryak, *Crystallogr. Rep.* **45,** 13–20 (2000).
20. A. A. Belik, V. B. Gutan, L. N. Ivanov, and B. I. Lazoryak, *Russ. J. Inorg. Chem.* **46,** 785–792 (2001).
21. A. A. Belik, V. A. Morozov, S. S. Khasanov, and B. I. Lazoryak, *Mater. Res. Bull.* **34,** 883–893 (1999).
22. R. Gopal, C. Calvo, J. Ito, and W. K. Sabine, *Can. J. Chem.* **52,** 1155–1164 (1974).
23. E. Kostiner and J. R. Rea, *Acta Crystallogr. B* **32,** 250–253 (1976).
24. B. I. Lazoryak, V. A. Morozov, A. A. Belik, S. Yu. Stefanovich, V. V. Grebenev, I. A. Leonidov, E. B. Mitberg, S. A. Davydov, O. I. Lebedev, and G. Van Tendeloo, *Chem. Mater.*, submitted.
25. V. A. Morozov, A. A. Belik, S. Yu. Stefanovich, V. V. Grebenev, O. I. Lebedev, G. Van Tendeloo, and B. I. Lazoryak, *J. Solid State Chem.* **165,** 278–288 (2002), doi:10.1006/jssc.2001.9521.
26. B. I. Lazoryak, V. A. Morozov, M. S. Safonov, and S. S. Khasanov, *Mater. Res. Bull.* **30,** 1269–1275 (1995).
27. B. I. Lazoryak, V. A. Morozov, and A. N. Zhdanova, RF Patent 95100507/26, 1995.
28. S. N. Britvin, Ya. A. Pakhomovskii, A. N. Bogdanova, and V. I. Skiba, *Can. Mineral.* **29,** 87–93 (1991).
29. J. F. Sarver, M. V. Hoffman, and F. A. Hummel, *J. Electrochem. Soc.* **108,** 1103–1110 (1961).
30. A. Bigi, E. Foresti, M. Gandolfi, M. Gazzano, and N. Roveri, *J. Inorg. Biochem.* **66,** 259–265 (1997).
31. A. A. Belik, F. Izumi, S. Yu. Stefanovich, A. P. Malakho, B. I. Lazoryak, I. A. Leonidov, O. N. Leonidova, and S. A. Davydov, *Chem. Mater.* **14,** 3197–3205 (2002).
32. J. R. Looney and J. J. Brown Jr., *J. Electrochem. Soc.* **118,** 470–473 (1971).
33. A. A. Belik, F. Izumi, T. Ikeda, B. I. Lazoryak, V. A. Morozov, A. P. Malakho, S. Yu. Stefanovich, V. V. Grebenev, O. V. Shelmenkova, T. Kamiyama, K. Oikawa, I. A. Leonidov, O. N. Leonidova, and S. A. Davydov, *Phosphorus, Sulfur Silicon* **177,** 1899–1902 (2002).
34. A. A. Belik, A. P. Malakho, B. I. Lazoryak, and S. S. Khasanov, *J. Solid State Chem.* **163,** 121–131 (2002), doi:10.1006/jssc.2001.9380.
35. A. A. Belik, B. I. Lazoryak, K. V. Pokholok, T. P. Terekhina, I. A. Leonidov, E. B. Mitberg, V. V. Karelina, and D. G. Kellerman, *J. Solid State Chem.* **162,** 113–121 (2001), doi:10.1006/jssc.2001.9363.
36. F. Izumi and T. Ikeda, *Mater. Sci. Forum* **321–324,** 198–204 (2000).
37. H. Toraya, *J. Appl. Crystallogr.* **23,** 485–491 (1990).
38. C. Dong, *J. Appl. Crystallogr.* **32,** 838 (1999).
39. "International Tables for Crystallography," (A. J. C. Wilson and E. Prince, Eds.), Vol. C, 2nd ed., pp. 572–574. Kluwer, Dordrecht, 1999.
40. L. Kissel, and R. H. Pratt, *Acta Crystallogr. A* **46,** 170–175 (1990).
41. "International Tables for Crystallography," (T. Hahn, Ed.), Vol. A, 4th ed. Kluwer, Dordrecht, 1996.
42. R. D. Shannon, *Acta Crystallogr. A* **32,** 751–767 (1976).
43. V. A. Morozov *et al.*, unpublished work.